Proceedings World Geothermal Congress 2026
Calgary, Canada, June 8 – 11, 2026

Time-Lapse Gravity Monitoring Insights into Exploitation Signatures at Lumut Balai Geothermal Field, Indonesia (2019-2024)

Astha Dandari Kusuma Wardhani[1], R. M. Tofan Sastranegara[1], Helmy Rizki Fauzi[1], M. Afif Habiburrahman[1] and Didi Darmadi[1]

PT Pertamina Geothermal Energy, Tbk[1]

astha.dandari@pertamina.com

Keywords: time-lapse, microgravity, gravity, monitoring, geothermal, Lumut Balai

ABSTRACT

A time-lapse gravity study was undertaken to characterize reservoir behavior at the liquid-dominated Lumut Balai geothermal field, Indonesia, across a pre-production baseline (2017-2019) and five years of the 55 MW Unit 1 production (2019-2024). Gravity monitoring allows for the detection of reservoir mass changes induced by geothermal fluid production and reinjection, as reflected by gravity changes over time. Baseline variations were minimal, reflecting natural background signals, whereas post-production signals evolved into pronounced negative anomalies over the production area and extending north–northeast, indicating progressive mass depletion associated with sustained fluid extraction. Three-dimensional density change inversion refines this geometry, showing down-structure, depth-increasing depletion beneath production area, localized positive at the northern reinjection area, and a broad positive to the south coinciding with the upland area and the system's upflow zone, suggesting natural recharge, likely deep-thermal fluids with possible meteoric contribution. Reservoir mass balance estimates indicate a modest mass deficit of ~8 to 9.6 Mt over 2019-2024 (~1.5 to 1.9 Mt per year) within the 8.6 km^2 control area, with an effective reservoir thickness of ~2.5 km. Approximately 91% of produced mass was replenished, largely by natural recharge supplemented by reinjection return, implying good reservoir-recharge connectivity. The nearly closed mass balance suggests that Lumut Balai Unit 1 is relatively well sustained by the current pressure support. This study further underscores the essential role of gravity monitoring in improving understanding of reservoir behavior, thereby strengthening the basis for sustainable reservoir management and future capacity growth at Lumut Balai.

1 INTRODUCTION

The application of geophysical monitoring techniques during geothermal utilization is important as they enable the observation and evaluation of reservoir dynamics over time. Changes in fluid pressure, temperature, and flow rate can lead to physical changes of fluid and reservoir rock properties, which can be detected using techniques such as microseismic velocity tomography, seismic amplitude attenuation, gravity, resistivity and magnetic field change monitoring, surface heat-loss remote sensing, and ground deformation mapping (Bromley, 2018). Numerous studies demonstrate that geophysical monitoring techniques refine the characterization of subsurface process, provide constraints that improve reservoir simulation models and contribute to reservoir management strategy.

Gravity monitoring, or time-lapse gravity, or microgravity, has been widely applied in geothermal fields to detect reservoir changes in subsurface mass which are reflected by gravity changes with time. Mass displacement can cause gravity change by their direct gravitational effect and by deformations at the Earth's surface (Torge, 1989). In geothermal systems, such displacements may result from natural processes (e.g., tectonic or volcanic activity) and/or from artificial processes, particularly fluid extraction and reinjection. The applications of gravity for geothermal reservoir monitoring have been published, such as for Wairakei, New Zealand by Allis and Hunt (1986), Hunt (1995), Hunt and Graham (2009); for Salak, Indonesia by Nordquist et al. (2010); and for Reykjanes, SW-Iceland by Gudnason et al. (2015). Three-dimensional inversion of time-lapse gravity data has also been successfully applied at Kamojang (Agung et al., 2018) and "US" field (Haq et al., 2019). Previous studies have demonstrated that development-related gravity changes in geothermal reservoirs primarily reflect changes in the distribution and phase state of reservoir fluids. In liquid-dominated reservoirs, production-induced gravity variations are driven mainly by shifts in the liquid–vapor distribution at depth, with gravity decreasing when steam and/or gas displaces water during early pressure drawdown and increasing when water re-saturates previously unsaturated zones (Allis et al., 2000). For vapor-dominated system, gravity decreases are mainly caused by reservoir dry-out, where steam-pressure drawdown boils residual liquid (Allis et al., 2000).

The Lumut Balai geothermal field is a high temperature- liquid-dominated geothermal system with temperature of 220°-260°C, located in Muara Enim Regency, South Sumatra Province in Indonesia. Geologically, Lumut Balai geothermal system lies within the 9-km-wide Old Lumut Caldera, about 60 km east of the Komering Segment, on eastern side of the Great Sumatra fault (Nurseto, 2021). As this paper was written, the Lumut Balai geothermal field has been generating electricity with an installed capacity of 1 × 55 MW from Unit 1 which began operation in September 2019. An additional 55 MW power plant, Unit 2, was projected to begin operation in mid-2025, and has since commenced operation. The location of the Lumut Balai is displayed in Figure 1.

Over five years of continuous Unit 1 production and reinjection at Lumut Balai field, PGE has conducted geophysical monitoring including microgravity, elevation changes (ground deformation), and microseismic observations. Baseline microgravity and elevation surveys were completed in 2017 and 2019, respectively, prior to plant commissioning in September 2019, and have since served as reference datasets for subsequent annual monitoring. This study analyzes time-lapse microgravity data from 2017 to 2024 and applies 3-D inversion to resolve density changes associated with Unit 1 operation. In addition to understanding the reservoir change associated with Unit 1, the findings are expected to provide insights for Unit 2 development.

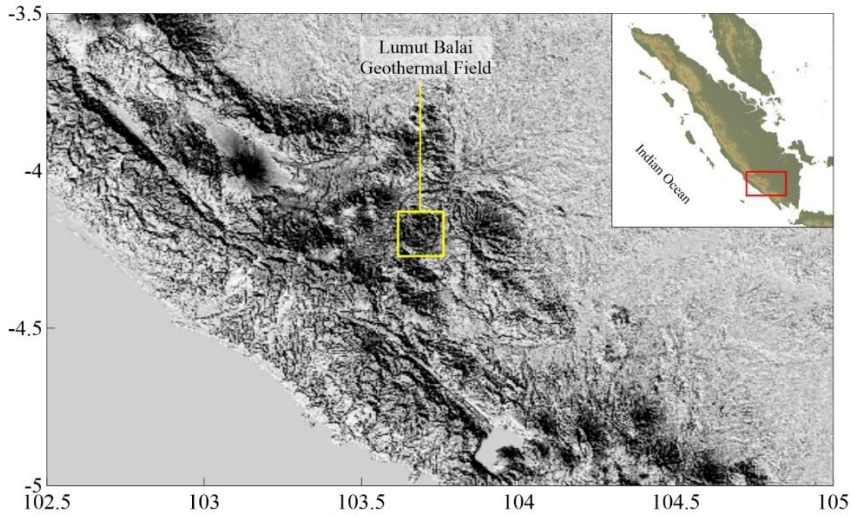


Figure 1: Location of the Lumut Balai field (yellow rectangle) in South Sumatra. The inset shows Sumatra Island with the zoomed-in area indicated by a red rectangle.

2 DATA AND METHOD

2.1 Gravity Data

Gravity monitoring is principally performed by repeated measurements at fixed points (benchmarks) over periods. Gravity measurements for monitoring in Lumut Balai have been carried out annually since 2017 until 2024, with exceptions in 2018 and 2022. The first measurement, serving as a baseline was conducted in July 2017 and was followed by a second measurement in March 2019, which is 5 months the power plant commenced operation in September 2019.

The gravity monitoring network in Lumut Balai spans an area of about 96 km^2, with benchmarks distributed across the production and reinjection area as illustrated in Figure 2. The number of gravity benchmarks varied from 69 to 102 over the years, as new stations were added to improve spatial coverage. All points were tied to the regional reference benchmark R1, located about 6 km to the north which is assumed to be unaffected by geothermal operation at Lumut Balai. The reliability of the observed gravity data was ensured through quality control and corrections for tidal effect and instrument drift. At each benchmark, gravity measurements were recorded for a sufficient duration to obtain stable readings. Quality control parameters included standard deviation, tilt, drift, and repeatability at each point.

To account for the gravity signal associated with mass displacement due to geothermal utilization, corrections were made for gravity effect from ground deformation and groundwater level changes. Accordingly, supplementary measurements were obtained, involving precise elevation surveys and groundwater level monitoring. The precise elevation measurements were carried out simultaneously with gravity data acquisition at the same benchmarks, while groundwater levels data were collected from a very few available shallow wells.

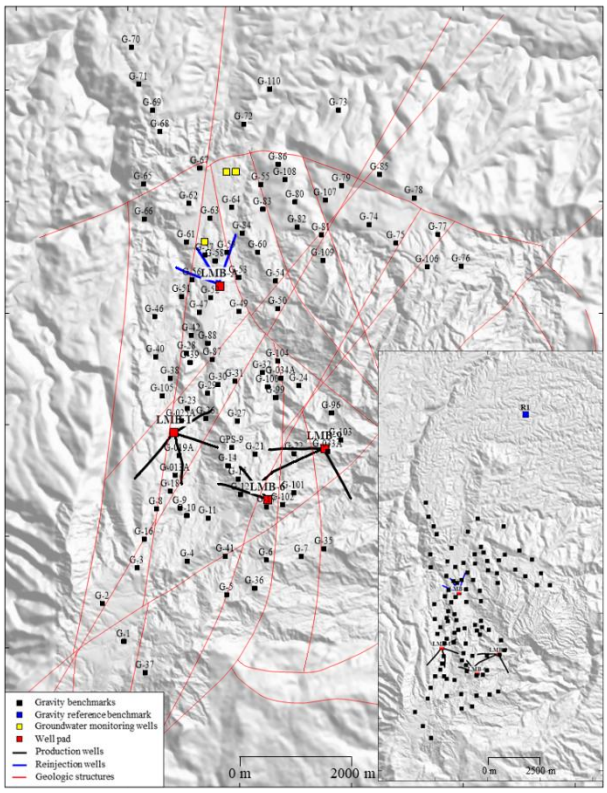


Figure 2: Locations of gravity monitoring benchmarks (black squares), and their location relative to regional reference point R1 (blue square) in the inset. Groundwater monitoring wells are marked with yellow squares. Production and reinjection wells are indicated by black and blue lines. Only wells relevant to this analysis are shown.

2.2 Production & Reinjection Data

The Lumut Balai Unit 1 produces geothermal fluid from nine production wells located on pads LMB-1, LMB-6, and LMB-9. The brine is reinjected into the reservoir through three reinjection wells on pad LMB-A. The layout of the production and reinjection wells is depicted in Figure 2.

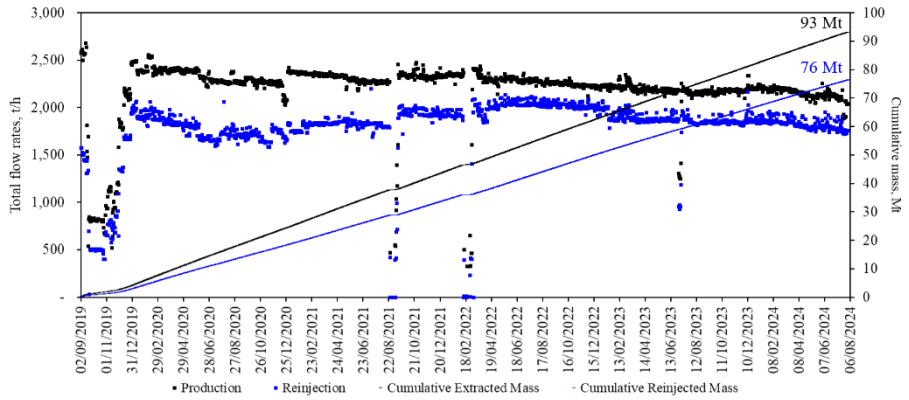


Figure 3: Lumut Balai Unit 1: the primary axis illustrates daily total production and reinjection flow rates in tonnes per hour (t/h), whereas the secondary axis indicates the approximate cumulative mass of production and reinjection in megatonnes (Mt) from September 2019 to July 2024.

In addition to gravity monitoring data, production and reinjection mass data from the wells were utilized to estimate the mass balance of the exploited reservoir. Figure 3 presents the daily total production and reinjection flow rates, along with the cumulative mass of both production and reinjection. Overall, there were no significant changes in production or reinjection trends during five years of operation at Lumut Balai. A noticeable increase occurred only between September and December 2019, corresponding to the early stage of the power plant's operation. Despite fluctuations, the overall production trend shows a gradual decline, with total flow rates decreasing by approximately 500 t/h over five years. As of July 2024, the total mass produced by Unit 1 reached

93 Mt (about 18-19 Mt per year), while the total reinjected mass was 76 Mt, indicating that about 82% of the extracted mass was returned to the reservoir.

2.3 Method

Basically, time-lapse gravity monitoring is a subtraction of observed gravity data at one year from the data of the previous year. Based on data availability, five periods of observed gravity changes were obtained: 2017-2019, 2019-2020, 2020-2021, 2021-2023, and 2023-2024.

To isolate signals associated with geothermal utilization, the observed gravity changes were corrected for elevation and groundwater level changes. In the case of the effect of elevation changes, the study applied the free-air correction formula to derive the gravity effect due to elevation change Δg_h (mGal) which is given by

$$\Delta g_h = -0.3086\,\Delta h \tag{1}$$

where Δh is elevation changes in meter (m). This means that elevation change of 1 cm contributes to a gravity change of 3.086 μGal. The elevation change correction was applied at all benchmarks.

The gravity effect of groundwater level changes can be estimated as a first approximation for uniform changes in homogeneous horizontal layers through a Bouguer plate model (Torge, 1989) of which Bouguer plate reduction Δg_b (m/s^2) is defined by

$$\Delta g_b = 2\,\pi\,G\,\rho\,h \tag{2}$$

where G is the Gravitational Constant (6.67 ×10^{-11} m^3 kg^{-1} s^{-2}), ρ is density (kg/m^3), and h is thickness (m). By using equation (2), the effect of groundwater level change Δg_{gw} (mGal) is given by

$$\Delta g_{gw} = (2\,\pi\,G\,\rho_w\,P\,\Delta h)\,\times 10^5 \tag{3}$$

where ρ_w is water density (kg/m^3), P is the fraction of water-filled pore space ($\emptyset S_w$) and Δh is groundwater level change (m). The water density is assumed to be 1,000 kg/m^3. Given the shallow groundwater depth, the porosity is assumed to be higher than in the reservoir as the near-surface materials are generally less consolidated. Hence, here, it is assumed that P is 0.25. This means that a groundwater level change of 1 m contributes to a gravity change of ~10 μGal. This number is generally accepted with reference to Allis and Hunt (1986). However, in the Lumut Balai geothermal field, groundwater level changes were observed to be minor, typically under 1 meter, and were therefore considered negligible. Nonetheless, this simplification could introduce uncertainty, as groundwater monitoring wells may not adequately represent variations across the broader area.

To investigate subsurface mass changes within the reservoir, cumulative gravity changes from 2019-2024 were analyzed. Cumulative gravity maps were generated using the grid-summation technique, allowing datasets from different years to be incorporated consistently. The 2019-2024 data was then inverted in 3-D using VOXI Earth Modelling Extension in Oasis Montaj software to obtain a density change model. For reservoir-scale imaging, the base of the clay cap was defined as the top boundary of the inversion mesh, assuming negligible mass change within the cap. Hence, the resulting anomaly represents density and mass changes within the reservoir beneath the clay cap.

Total mass change ΔM was then obtained simply by calculating the total density change of a defined volume, which is given by

$$\Delta M = \sum_{i=1}^{n} (\Delta\rho_i\,V_i) \tag{4}$$

where density change $\Delta\rho$ is expressed in kg/m^3, volume V in m^3, and n is the total number of density changes cube from the 3-D model.

Mass change derived from the 3-D density changes model was then cross-validated using Gauss's theorem, which provides an independent estimate of mass displacement from the observed gravity data. Even though interpretation of gravity measurements is not unique in determining the distribution of anomalous masses, they can provide an estimate of the total anomalous mass which is corollary of Gauss's flux theorem in potential theory (Parasnis, 1986) which is given by

$$\Delta M = \frac{1}{2\pi G} \iint \Delta g\; dS \tag{5}$$

where Δg is expressed in m/s^2, the surface area element dS in m^2 and ΔM is in kg.

For ΔM in Mt, thus

$$\Delta M = 2.39 \sum_{i=1}^{n} (\Delta g_i \Delta S_i) \quad (6)$$

where Δg is expressed in μGal, the surface area element ΔS in km^2.

The estimate of ΔM in Equation (6) is in some way an underestimate because it is common practices to apply summation in integration over a finite area, while on the contrary, ΔM in equation (5) is over an infinite area (Parasnis, 1986). For the Gauss calculation, a MATLAB-based program developed by PGE was used.

Finally, the reservoir mass balance was assessed by integrating the gravity-derived mass change within the defined control area with the corresponding production and reinjection volumes over the monitoring period.

3 RESULT AND DISCUSSION

3.1 Data Uncertainty

Uncertainties were evaluated to assess the reliability of the gravity monitoring data, including gravity and elevation measurement accuracy, groundwater level variation, and benchmark stability. The uncertainty in gravity measurements, represented by the mean standard deviation, ranges from 1 to 5 μGal, while that from elevation accuracy is 2 to 5 μGal. Groundwater level monitoring, which is ideally included at each control point to correct for its effect, is limited to a very few shallow wells and thus not adequately represent the spatial variability across the study area. The uncertainty resulting from this limitation is estimated to range from 1 to 10 μGal, given that groundwater level variation in the area is less than 1 m. Benchmarks, constructed in concrete due to the absence of exposed bedrock in Lumut Balai, are less stable than natural bedrock and therefore more prone to deformation. This condition may introduce uncertainties that cannot be directly quantified. Overall, the total uncertainty is reasonably estimated to be up to ±20 μGal.

3.2 Gravity Change Analysis

Gravity changes were analyzed for both the pre-operational baseline 2017-2019 and as cumulative changes referenced to 2019 for the subsequent monitoring intervals through 2024. The gravity changes maps shown in Figure 4 illustrate the transition from pre-operation stability observed in 2017-2019 to dynamic mass redistribution during the operational phase, as reflected in the periods 2019-2021, 2019-2023, and 2019-2024.

The 2017-2019 period represents the baseline state prior to Unit 1 power plant operation. Gravity changes during this period were minimal, reflecting only natural variations in the subsurface which is in the range of -25 to +10 μGal. This baseline serves as the reference for subsequent gravity changes associated with Unit 1 operation.

Following the commencement of Unit 1 production in September 2019, time-lapse gravity monitoring reveals clear signatures of reservoir response. In 2019-2021, more distinct gravity changes anomaly developed, with negative values reaching approximately -30 μGal around production wells and positive values up to +25 μGal near the reinjection wells. This pattern reflects the immediate subsurface response to fluid extraction and reinjection, with mass depletion occurring in the production area and localized mass addition in the reinjection area. The depleted zone associated with production during this period showed only minor changes compared to the pre-operation condition, possibly sustained by pressure support from northern reinjection wells and natural recharge particularly from the south, as indicated by a positive anomaly of up to +30 μGal in that area. From 2019 to 2023, the negative anomalies became more pronounced, reaching about -50 μGal, indicating progressive mass depletion due to continuous fluid withdrawal. The 2019-2024 period represents the most recent condition after five years of exploitation, showing further development of these anomalies, with negative anomalies in the production area intensifying to -100 μGal and expanding northward and northeastward, reflecting a more significant mass depletion over time. While negative gravity changes in liquid-dominated reservoirs are mainly attributed to the conversion of liquid water to steam, this mechanism is not strongly supported at Lumut Balai, as well-monitoring records from pads LMB-1, LMB-6, and LMB-9 show no significant increase in steam fraction or dryness, which has remained essentially stable throughout the study period.

Figure 5 presents the time series of gravity changes observed at benchmarks G-4, G-22, and G-61, all showing a decreasing gravity trend. At benchmark G-61 in the northern sector where reinjection exists, the maximum gravity decrease is -50 μGal, consistent with the pressure support and partial mass compensation from reinjection. In contrast, G-22 within the production area exhibits a larger gravity decrease of -90 μGal, indicating continuous mass depletion near active production wells. In the southern sector where no reinjection occurs, G-4 records a smaller decrease of -30 μGal, implying that the mass loss in this sector is possibly offset by natural recharge. These spatial patterns align with the south-to-north hydrology flow at Lumut Balai.

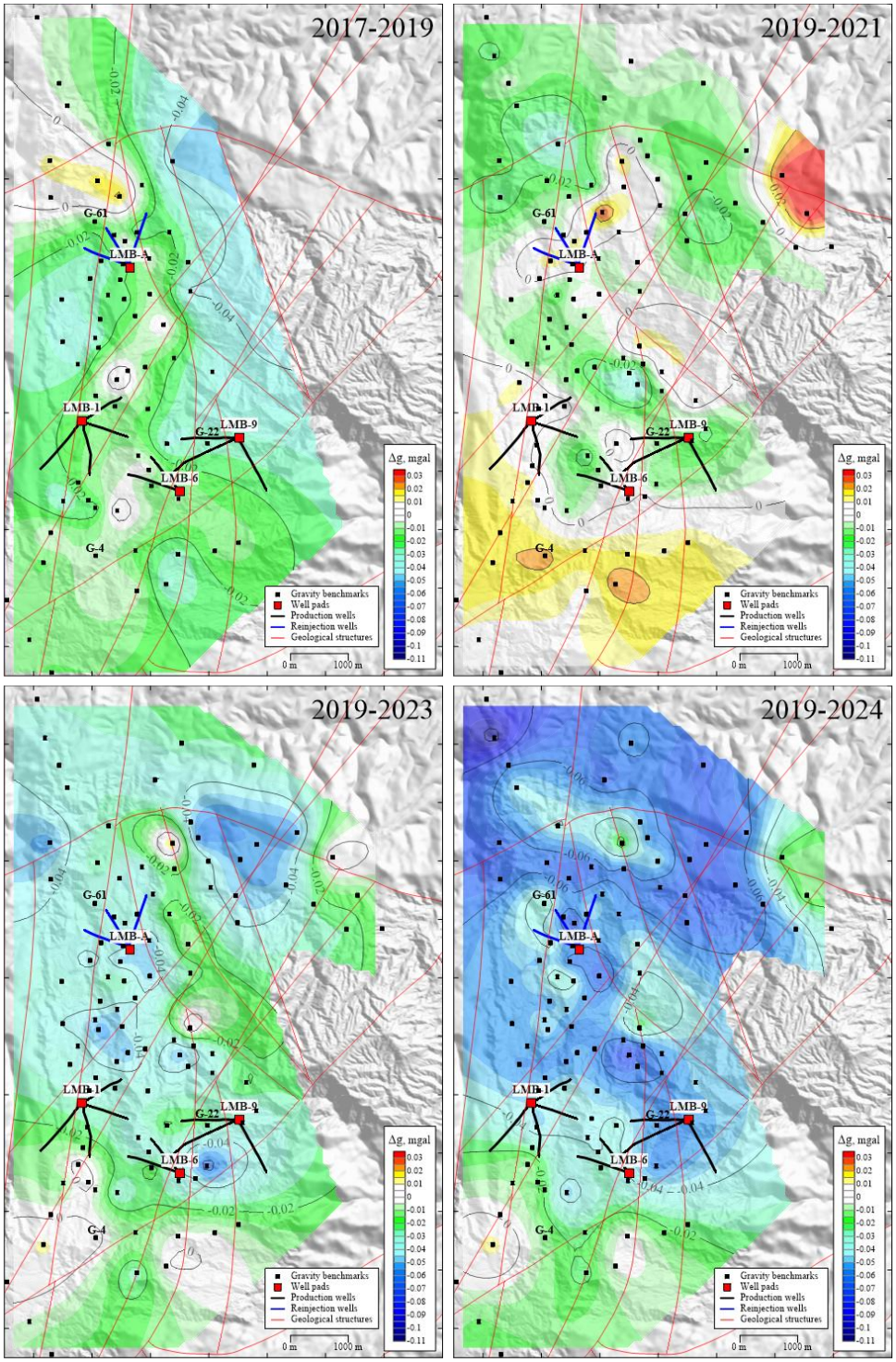


Figure 4: Gravity change maps showing temporal variations in the Lumut Balai. The 2017–2019 map represents the pre-operation baseline, while the subsequent maps (2019–2021, 2019–2023, and 2019–2024) illustrate the evolution of gravity change associated with production and reinjection activity. Only wells relevant to this analysis are shown.

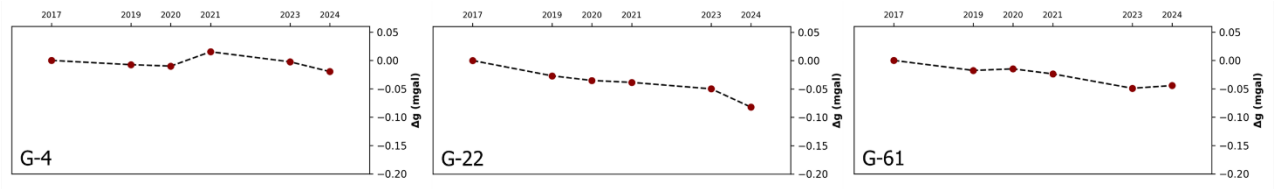


Figure 5: Time series of gravity change at benchmarks G-4 (southern sector), G-22 (production area), and G-61 (northern reinjection area). Benchmark locations are shown in Figure 4.

3.3 The 3-D Density Change Model Analysis

A 3-D inversion of time-lapse gravity data for 2019-2024 resolves subsurface density perturbations spanning -0.009 to +0.014 g/cm^3, providing insights into the reservoir response to prolonged production and reinjection activities. Figure 6 displays horizontal slices at 0 m, -400 m, -800 m, and -1200 m above sea level (asl) and Figure 7 presents vertical profiles across the reservoir. Red anomaly represents density increases, while blue anomaly indicates density decreases. Across the horizontal slices, density change patterns evolve from patchy signals at shallow levels to strong laterally coherent anomalies at depth.

Compared with the 2019-2024 gravity change map, the density change model exhibits stronger lateral contrast and more clearly delineates the most depleted reservoir area. Negative density change dominates in the production area, spreading down-structure and enlarging with depth, consistent with pressure drawdown and sustained fluid withdrawal from production wells at LMB-1, LMB-6, and LMB-9. Localized positive density change around reinjection wells at LMB-A corresponds to mass addition and cooling-related densification. The southward tendency of this positive anomaly suggests connection toward the producing area, implying that reinjection partly compensates for production-related mass loss. The negative density changes in the northern sector, despite the absence of production wells, possibly associates with connectivity to the southern production block where drawdown propagates northward and drives lateral drainage. However, inversion-related uncertainties remain that could bias amplitudes and geometry, therefore, additional evidence is advised.

In the southern sector where reinjection is absent, a broad positive density change coincides with the high elevation terrain and is interpreted as natural recharge introducing relatively denser fluid into the system. Its spatial correspondence with the inferred upflow zone at Lumut Dome supports an interpretation of deep thermal recharge, with possible contributions of local meteoric water induced by drawdown. Overall, the pattern implies south-to-north flow connectivity, with southern recharge and northern reinjection providing pressure support.

3.4 Reservoir Mass Balance

Reservoir mass balance was evaluated by integrating gravity-derived mass changes with production and reinjection data. Mass change from gravity was derived using two approaches: volumetric integration of 3-D density changes (Equation 4), and application of Gauss's theorem to the measured gravity change (Equation 6). The control area for mass balance assessment was defined as a 500 m buffer surrounding the production wells, excluding the reinjection wells, although reinjection inflow was still incorporated in the calculation. Because the actual reinjection return to the control area is uncertain, two comparison scenarios were considered. Scenario 1 adopts 3% of injected mass return, based on tracer test recovery at the production wells, and is considered as a pessimistic number. Scenario 2 assumes a more representative 50% return, acknowledging that complete (100%) return is unrealistic. For the density-based calculations, multiple reservoir thicknesses (1000, 1500, 2000, 2500, and 3000 m) were tested. Results of the mass change estimates are summarized in Table 1.

Table 1 shows that both mass balance approaches yield comparable net mass losses for 2019-2024, about 8 to 9.6 Mt (8.35 Mt by Gauss) within the control area of 8.6 km^2. Moreover, the Gauss estimate aligns most closely with the density-based result obtained using reservoir thickness of 2,500 m. This agreement cross-validates the two approaches and suggests that reservoir mass redistribution is likely concentrated within a ~2.5 km vertical column beneath the control area, which can be regarded as the effective reservoir thickness.

Over five years, with a total extraction of 93 Mt (averaging 18-19 Mt per year) and a cumulative mass deficit of 8.35 Mt (1.5-1.9 Mt per year), it implies that 84.7 Mt of mass was replaced through combined reinjection return and natural recharge. This indicates that approximately 91% of the produced mass was replenished. Calculations further suggest that natural recharge alone contributed between 46 to 83 Mt of inflow, providing substantial support for Unit 1 production. The relatively small mass deficit is consistent with the minor decline rate of ~0.5% per year reported by Yanto et al. (2022), indicating moderate and gradual reservoir depletion under effective pressure-maintenance conditions. This near-closed mass balance, largely driven by natural recharge, indicates significant connectivity between the reservoir and recharge sources, implying generally good permeability across the reservoir.

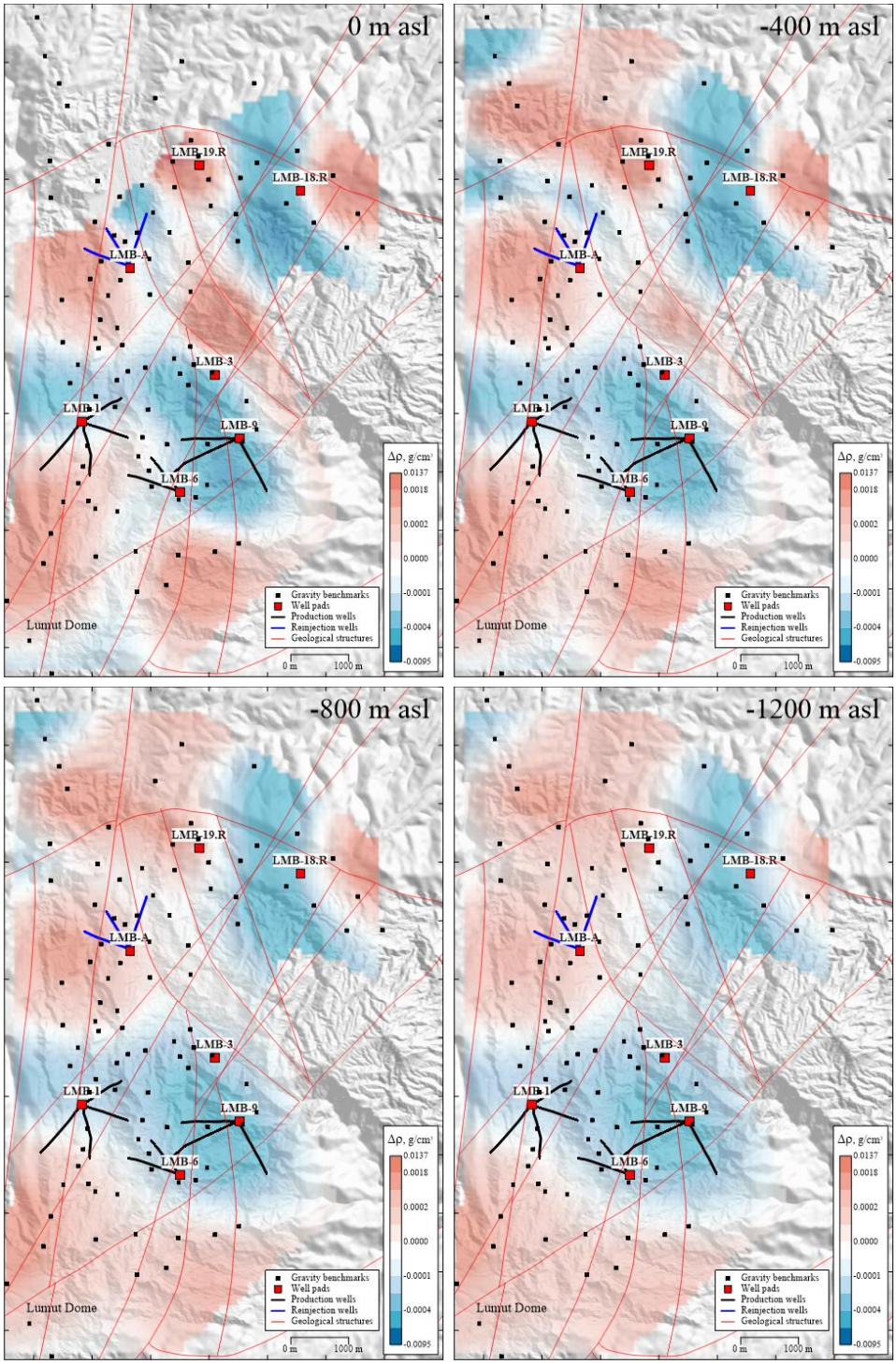


Figure 6: Density changes horizontal slices for the 2019-2024 period. Only wells relevant to this analysis are shown.

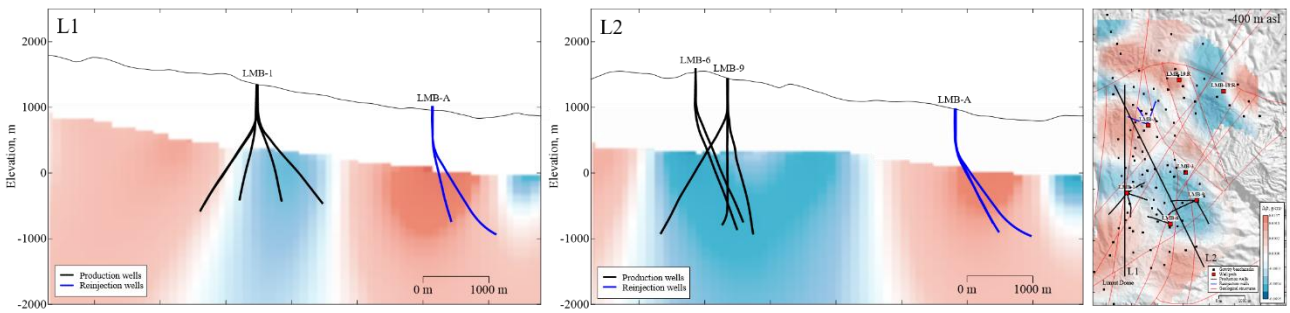


Figure 7: Density changes vertical profiles for the 2019-2024 period.

Table 1. Reservoir mass balance for 2019-2024. Positive values indicate mass addition; negative values indicate mass withdrawal. Total extraction = 93 Mt; total reinjection = 76 Mt.

Thickness (m)	Calculated mass change, (Mt)	Extraction (Mt)	Scenario 1		Scenario 2	
			Reinjection by 3% (Mt)	Recharge (Mt)[1]	Reinjection by 50% (Mt)	Recharge (Mt)[1]
Density Change Model						
1000	-3.95	-93	2.28	86.77	38	51.05
1500	-5.80			84.92		49.20
2000	-7.34			83.38		47.66
2500	-8.18			82.54		46.82
3000	-9.57			81.15		45.43
Gauss's Theorem						
	-8.35	-93	2.28	82.37	38	46.65

[1]Recharge = Calculated mass change − Extraction − Reinjection

3.5 Insights into the Upcoming Unit 2 Production

If a 55 MW Unit 2 is developed using production wells from pad LMB-3 (location shown in Figure 6), it would withdraw additional mass from a compartment that is already depleted, and converting LMB-A to production will likely expand this depletion. Output may rise initially but a more rapid decline is expected unless pressure support is enhanced. Increased production would deepen local drawdown, shift fluid-phase behavior (steam-cap development or gas breakout), change enthalpy, and promote subsidence risk. In terms of mass-balance, net mass loss would become more negative, resulting in larger gravity/density decreases and a faster pressure decline. Accordingly, an effective reinjection strategy is essential to help maintain reservoir pressures and sustain Unit 2 performance. New reinjection planned at pads LMB-18 and LMB-19 in the north (Figure 6) should help mitigate these impacts if effective flow paths connect to the depleted zone, with natural recharge contributing additional support.

Given the current estimates, the mass balance is nearly closed, with substantial natural recharge supplying most of the make-up mass, indicating strong connectivity between the reservoir and recharge sources, although it may not be uniformly across reservoir. This could favor Unit 2 in terms of potential mass and pressure support if the incoming natural recharge remains sufficiently hot to be effective. However, time-lapse gravity under Unit 1 still shows depletion, implying that natural recharge plus reinjection can help but may be insufficient on their own if production increases.

4 CONCLUSION

Time-lapse gravity at Lumut Balai delineates subsurface mass redistribution across the pre-production baseline and the 2019-2024 production period. Baseline (2017-2019) variations were minimal, reflecting natural background signals. After Unit 1 came online (September 2019), gravity evolved from modest changes to stronger negative anomalies reaching up to -100 µGal, indicating progressive depletion centered on production area and extending north-northeast. Density inversion confirms down-structure, depth-increasing depletion around production wells, with positive anomalies near the northern reinjection area. A broad positive anomaly in the south, aligned with the upland area and the system's upflow zone, suggests natural recharge, likely deep-thermal fluids with possible meteoric contribution. Overall, the gravity/density changes patterns imply south-to-north connectivity, with recharge in the south and reinjection in the north contributing to pressure support.

Reservoir mass balance estimates indicate a modest mass deficit of ~8 to 9.6 Mt over 2019-2024 (~1.5 to 1.9 Mt per year) within the 8.6 km^2 control area, with the Gauss result consistent with an effective reservoir thickness of ~2.5 km. Nearly 91% of the 93 Mt produced was replenished by ~84.7 Mt of inflow, most of it from natural recharge (~46-83 Mt) alongside reinjection return. This indicates meaningful reservoir-recharge connectivity and, by implication, generally good permeability. With its minor decline rate and nearly closed mass balance,

Lumut Balai Unit 1 appears to be relatively well supported by existing pressure support from natural recharge and reinjection.

Developing Unit 2 from LMB-3 and converting LMB-A would tap an already depleted compartment, yielding an initial increase in output but likely followed by a rapid decline unless pressure maintenance is enhanced. Although the reservoir mass balance under Unit 1 is nearly closed due to substantial natural recharge, this benefit helps only if the inflow is sufficiently hot and well connected to the target compartment. Sustained performance will require optimized and well-placed reinjection, confirmation of its connectivity through tracer interference tests, and supported by continued gravity and micro-seismic monitoring.

Acknowledgements

We would like to express our sincere gratitude to PT Pertamina Geothermal Energy, Tbk (PGE) for its support in carrying out this study as part of company's continuing efforts toward sustainable geothermal development and for granting permission to publish the result. Our appreciation is also extended to PGE's geoscience and reservoir team and to the reviewers for the valuable feedback, which helped in strengthening the discussion and improving the overall quality of this paper.

REFERENCES

Agung, L., Sastranegara, R.M.T., Hendriansyah, T., Nugroho, S.I., Firmansyah, W., Dandari, A., and Raharjo, I.B.: Kamojang Reservoir Mass Changes Revealed from The Application of Gauss Theorem to Microgravity Data during Periods 2016-2014, Proceedings The 2nd Southeast Asian Conference on Geophysics (SEAGC), Bali, Indonesia, (2018).

Allis, R.G., Gettings, P., and Chapman, D.S.: Precise Gravimetry and Geothermal Reservoir Management, Proceedings 25th Workshop on Geothermal Reservoir Engineering, Stanford University, California, (2000), 10 pp.

Allis, R.G., and Hunt, T.M.: Analysis of Exploitation-Induced Gravity Changes at Wairakei Geothermal Field, Geophysics, 51, 8, (1986), 1647-1660.

Bromley C.: The Role of Advanced Geophysical Monitoring in Improved Resource Expansion and Make-up Well Drilling Strategy, Proceedings 43rd Workshop on Geothermal Reservoir Engineering, Stanford University, California, (2018), 8 pp.

Gudnason, E.Á., Arnaldsson, A., Axelsson, G., Berthet, J.C.C., Halldórsdóttir, S., and Magnússon, I.T.: Analysis and Modelling of Gravity Changes in the Reykjanes Geothermal System in Iceland, During 2004-2010, Proceedings World Geothermal Congress 2015, Melbourne, Australia, (2015), 8 pp.

Haq, F.D., Sastranegara, T., Agung, L., Kusuma, A.D., Hendriansyah, T., Fanani, A.F., and Raharjo, I.B.: Production and Reinjection Evaluation on The Basis of 3-D Time-lapse Microgravity Inversion, IOP Conf. Ser.: Earth Environ. Sci., (2019), 318.

Hunt, T.M.: Microgravity Measurements at Wairakei Geothermal Field, New Zealand; A Review of 30 years data (1961-1991). Proceedings World Geothermal Congress 1995, Firenze, Italy, (1995), 6 pp.

Hunt, T.M., and Graham, D.J.: Gravity changes in the Tauhara sector of the Wairakei-Tauhara geothermal field, New Zealand, Geothermics, 38, 1, (2009), 108-106.

Nordquist, G.A., Acuna, J.A., and Stimac, J.: Precision Gravity Modeling and Interpretation at the Salak Geothermal Field, Indonesia, Proceedings World Geothermal Congress 2010, Bali, Indonesia, (2010), 8 pp.

Nurseto, S.T., Satriani, R.A.J., and Thamrin, M.H.: Geology of Lumut Balai Geothermal Field, Proceedings World Geothermal Congress 2010+1, Reykjavik, Iceland, (2021), 13 pp.

Parasnis, D.S.: Principles of Applied Geophysics (Fourth Edition), Chapman and Hall, New York, (1986), 412 pp.

Torge, W.: Gravimetry, De Gruyter, Berlin, (1989), 465 pp.

Yanto, E., Budiyanto, A., Tiofami, A., Marastio, F.E., Khasani, D., Budiman, P., and Suranto, H.: Analysis of Heat Recovery Time Predictions for Multiple Periods of Temporary Reinjection in Geothermal Well Production at Lumut Balai Field, Proceedings 45th New Zealand Geothermal Workshop, Auckland, New Zealand (2022), 7 pp.